NV center electronic state

NV center
(**sensor**)

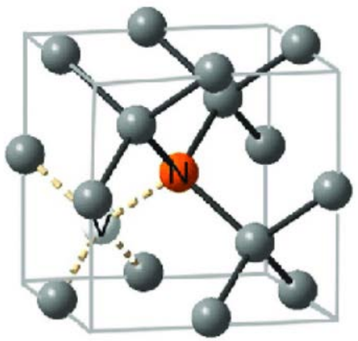

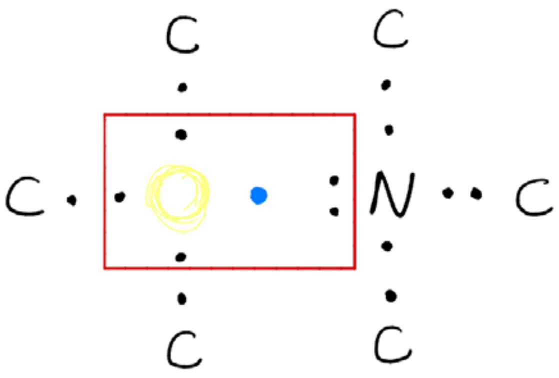

Structure of NV^-

vacancy

aditional electron

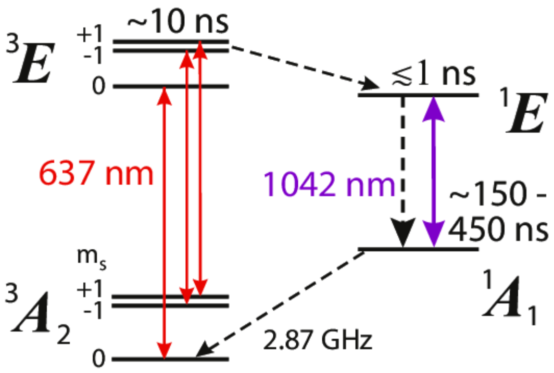

Energy level diagram of NV⁻⁻

negative **NV^-: S = 1**

neutral **NV^0: S = ½**

positive **NV^+: S = 0**

NV center electronic state

NV center
(**sensor**)

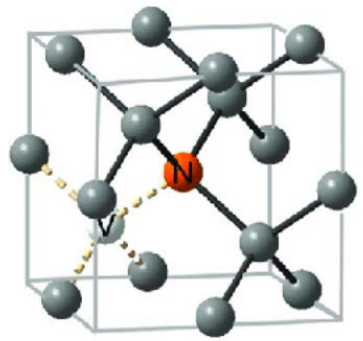

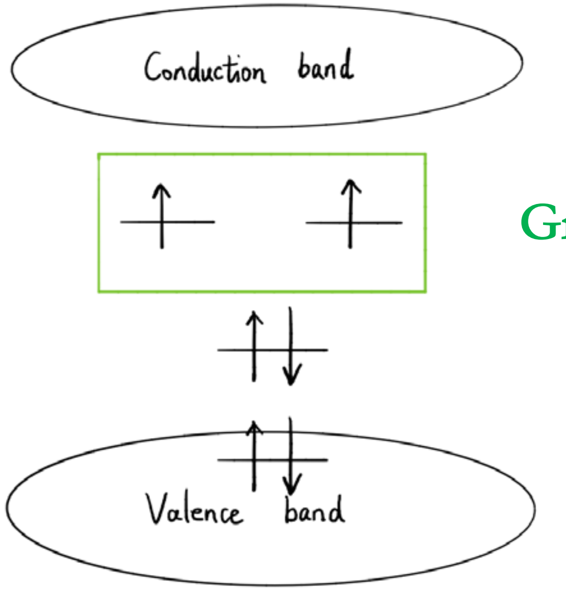

Ground state

Triplet
$$\begin{cases} \uparrow\uparrow = |1,1\rangle \\ \dfrac{\uparrow\downarrow+\downarrow\uparrow}{\sqrt{2}} = |1,0\rangle \\ \downarrow\downarrow = |1,-1\rangle \end{cases}$$

Singlet
$$\frac{\uparrow\downarrow-\downarrow\uparrow}{\sqrt{2}} = |0,0\rangle$$

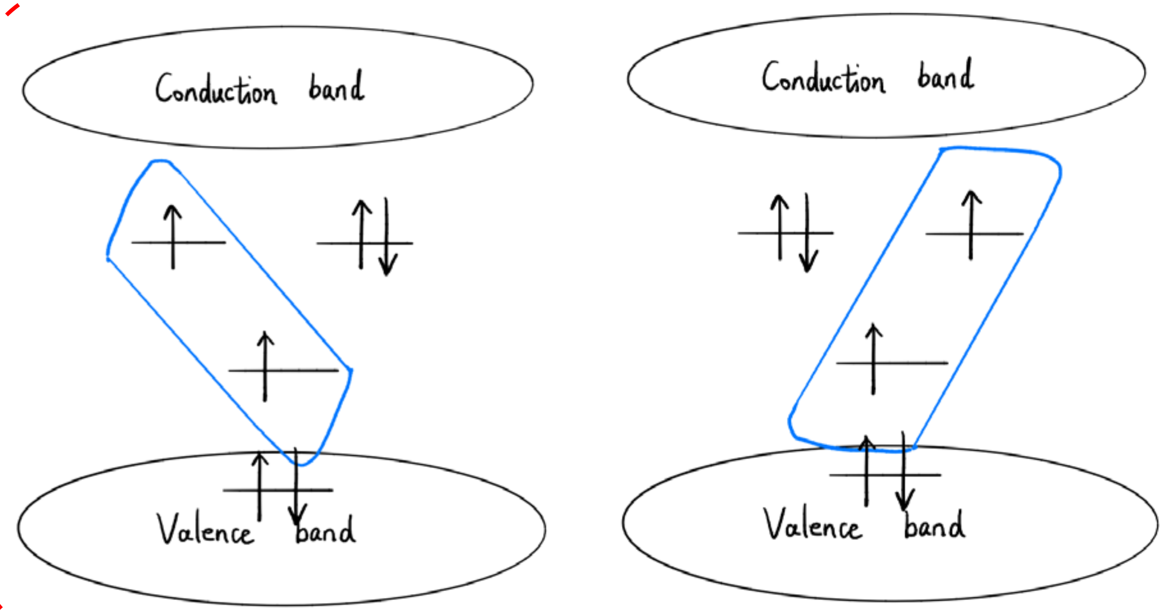

Excited state

NV center electronic state

Zero-filed H: SOC & spin-spin interaction

$$H_g = \frac{1}{\hbar}\left(\vec{S}\cdot\vec{D}\cdot\vec{S}\right)$$

Zero field splitting tensor $\vec{D} = \begin{pmatrix} D_{xx} & & \\ & D_{yy} & \\ & & D_{zz} \end{pmatrix}$

$$= \frac{1}{\hbar}\left(S_x D_{xx} S_x + S_y D_{yy} S_y + S_z D_{zz} S_z\right)$$

$$= \frac{1}{\hbar}\left(D_x S_x^2 + D_y S_y^2 + D_z S_z^2\right)$$

$S_z^2 = \begin{pmatrix} 1 & & \\ & 0 & \\ & & 1 \end{pmatrix}$ $S_x^2 = \begin{pmatrix} \frac{1}{2} & & \frac{1}{2} \\ & 1 & \\ \frac{1}{2} & & \frac{1}{2} \end{pmatrix}$ $S_y^2 = \begin{pmatrix} \frac{1}{2} & & -\frac{1}{2} \\ & 1 & \\ -\frac{1}{2} & & \frac{1}{2} \end{pmatrix}$

$D = \frac{3}{2}D_z,\ E = \frac{D_x - D_y}{2}$

D traceless

$$= \hbar\begin{pmatrix} \frac{D}{3} & & E \\ & -\frac{2}{3}D & \\ E & & \frac{D}{3} \end{pmatrix} = \hbar\left\{D\left[\hat{S}_z^2 - \frac{S(S+1)}{3}\right] + E\underbrace{\left(\hat{S}_+^2 + \hat{S}_-^2\right)}_{=\,2(S_x^2 - S_y^2)}\right\}$$

Ground state longitudinal and transverse zero-field splittings D_{GS} and E_{GS}

With energy & states:

$$-\frac{2}{3}D\hbar,\ \begin{pmatrix} 0 \\ 1 \\ 0 \end{pmatrix};\quad \left(\frac{D}{3} - E\right)\hbar,\ \begin{pmatrix} -1 \\ 0 \\ 1 \end{pmatrix};\quad \left(\frac{D}{3} + E\right)\hbar,\ \begin{pmatrix} 1 \\ 0 \\ 1 \end{pmatrix};$$

$|m_s = 0\rangle$ $\quad |-\rangle$ $\quad |+\rangle$

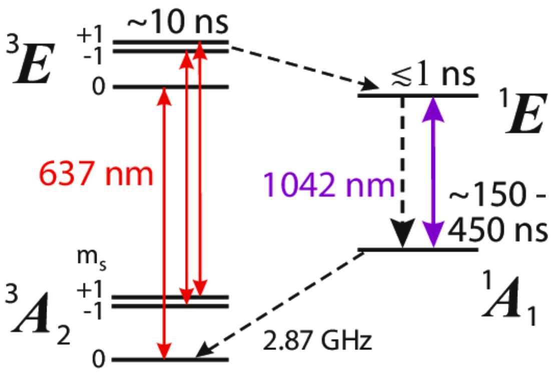

Energy level diagram of NV^{-}

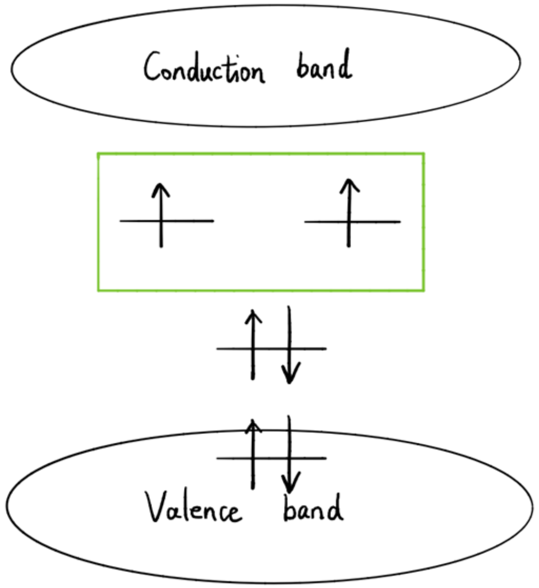

Coherent manipulation of NV center

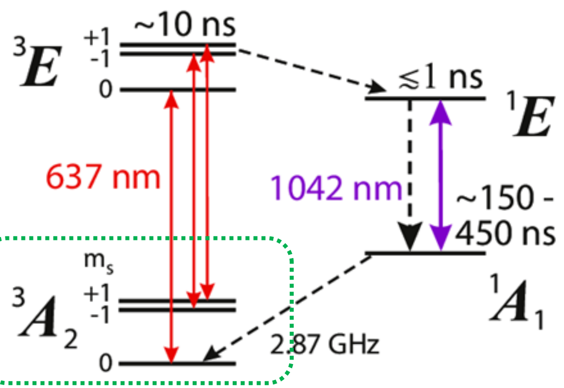

(Optical pump)

$$|m_s = 0\rangle \longrightarrow \frac{|0\rangle + |+\rangle}{\sqrt{2}} \longrightarrow \frac{1}{\sqrt{2}}\left(|0\rangle + e^{-i\phi}|+\rangle\right)$$

Governed by time-dependant $\vec{B}$

(MW) $\frac{\pi}{2}$ pulse

evolution

projection : fluorescence

$$H_{MW} = \gamma_e B_{AC} S_x \cos(\omega\tau)$$

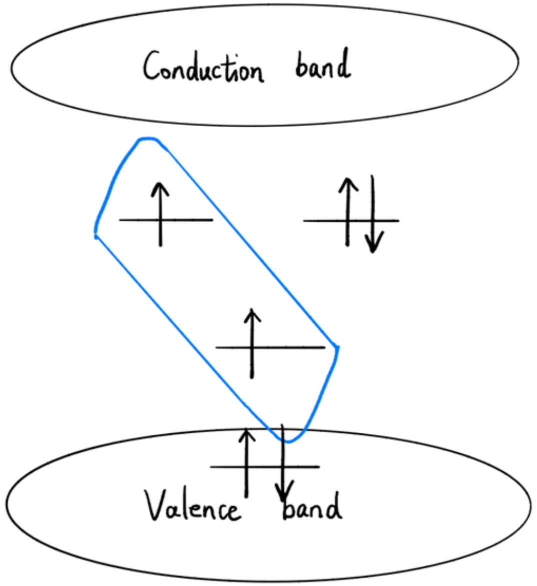

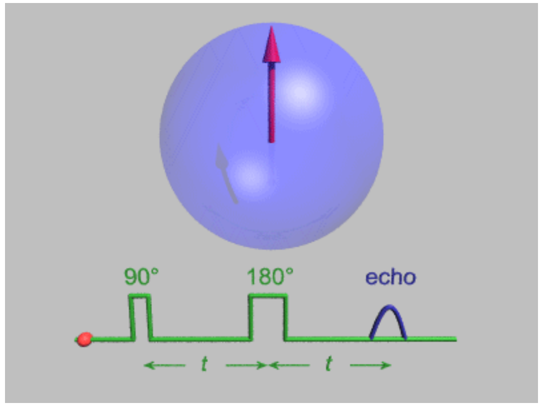

coherence is mapped by another $\pi/2$ pulse into a population difference

Echo amplitude ~ polarization difference

simplest form of dynamical decoupling

Traditional Nuclear Quadrupole Resonance (NQR)

↑

non-spherical nuclear charge
distributions for I ⩾ 1 nuclei

^{14}N, ^{17}O, ^{35}Cl, ^{63}Cu $\cdots$

Interact with EFG:
electric field gradient
(crystal field?)

Transition frequency for axial symmetry

Specific frequency
for a given system

$$\nu_Q = \frac{3e^2 \boxed{qQ}}{4I(2I-1)h}$$

Q: nuclear quadrupole moment

q ~ largest principal component of the EFG tensor at the nucleus

I: nuclear spin

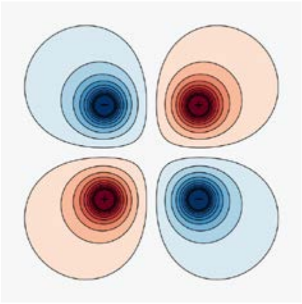

Charge = 0
Dipole moment = 0
Q ≠ 0

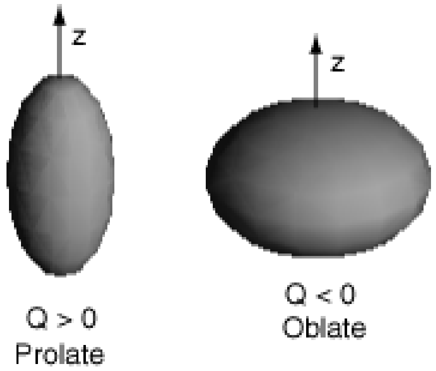

B. H. Suits, Handbook of Applied Solid State Spectroscopy (Springer, New York, USA, 2006).

NV center as a nanoscale NQR spectrometer

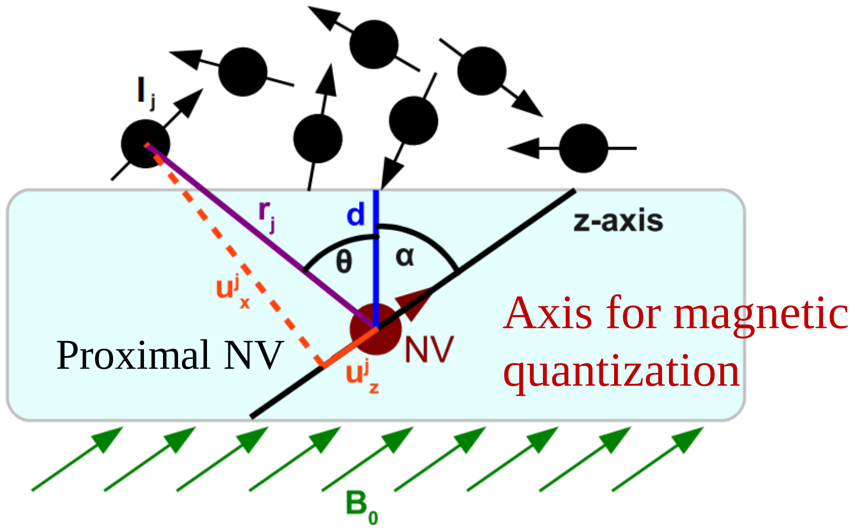

Measure statistical fluctuations of the spin polarization ~ $\sqrt{N}$
(independent of the applied field)

N: number of nuclear spins in the sensing volume

High sensitivity and small sensing volume:
ability to probe atomically thin layers

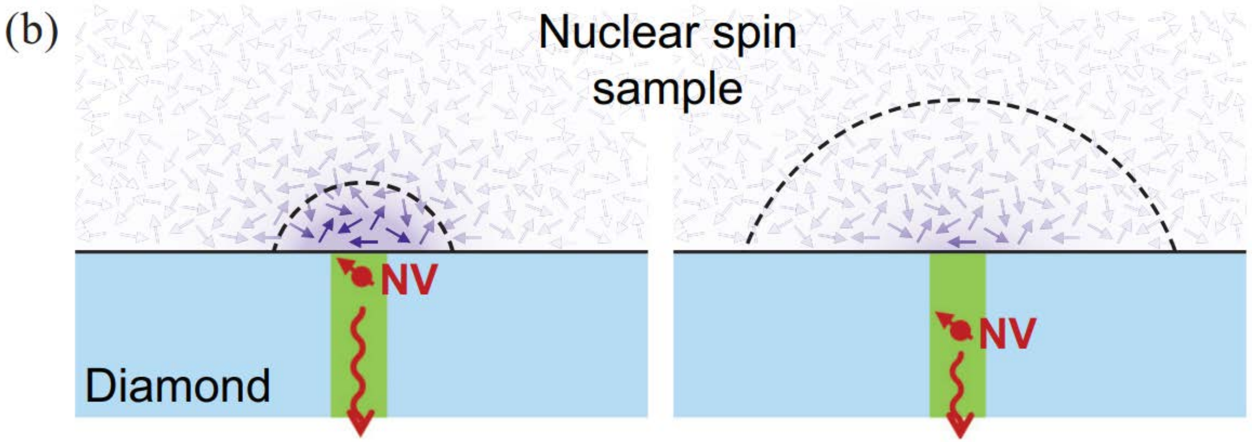

Depth: 6.8 ± 0.1 nm

Due to dipolar coupling, a shallow NV center experiences a significantly stronger magnetic field from a smaller nuclear spin sample volume than a deep NV center experiences.

NMR technique for determining the depth of shallow nitrogen-vacancy centers in diamond
Linh M. Pham, Stephen J. DeVience et al

Special case: h-BN flake

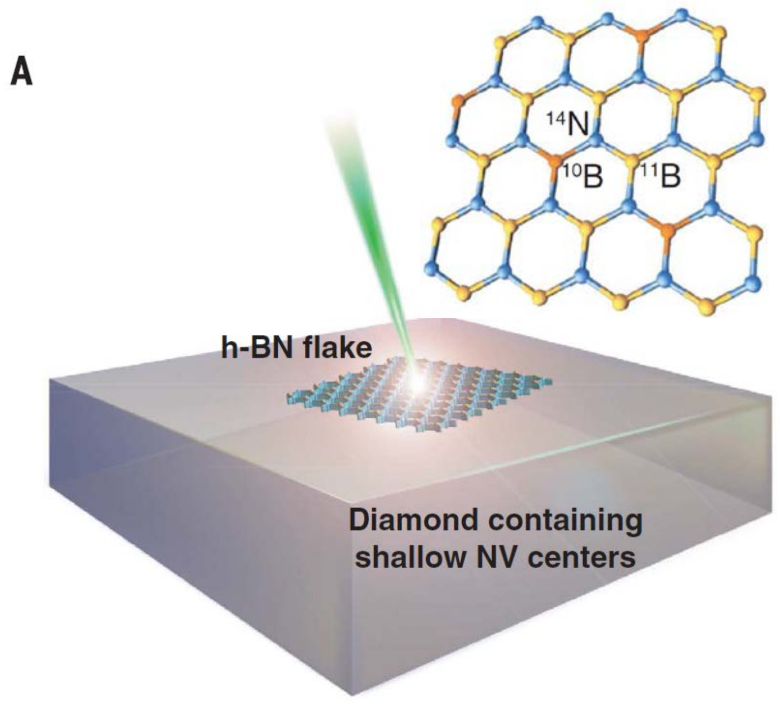

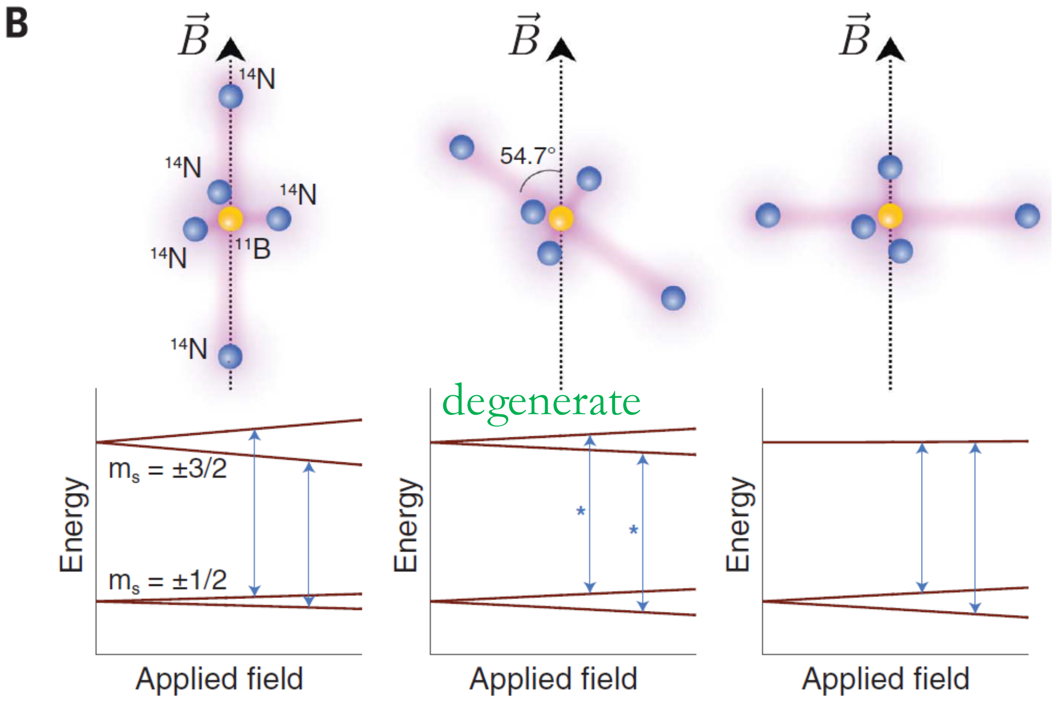

m_I = -I, -I+1, …, I-1, I

I = 3/2 I = 3

(80% ^{11}B, 20% ^{10}B)

(close to 100% ^{14}N) I = 1

honeycomb layered structure

$$E_{\pm 3/2} = h\nu_Q \left(1+\frac{\eta^2}{3}\right)^{1/2}$$

$$E_{\pm 1/2} = -h\nu_Q \left(1+\frac{\eta^2}{3}\right)^{1/2}$$

B. H. Suits, Handbook of Applied Solid State Spectroscopy (Springer, New York, USA, 2006).

Special case: h-BN flake

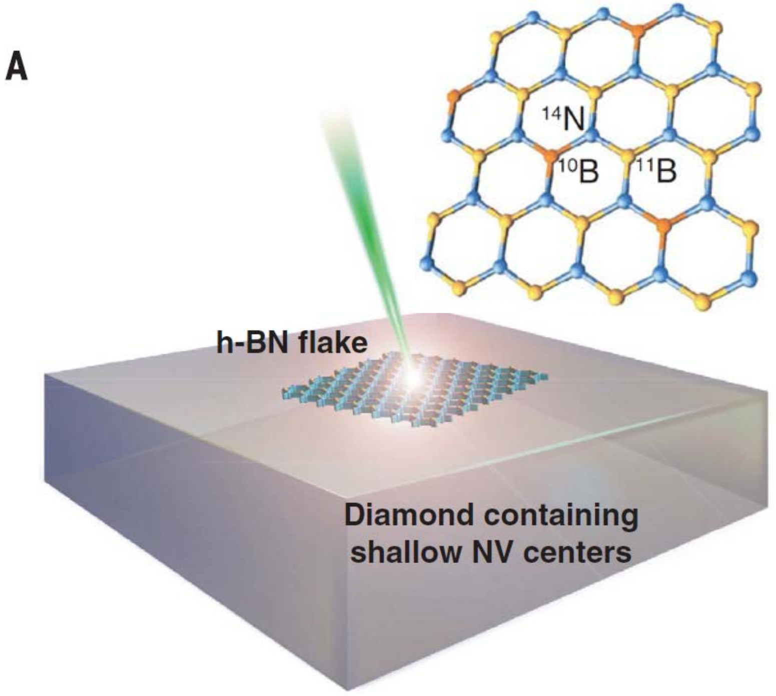

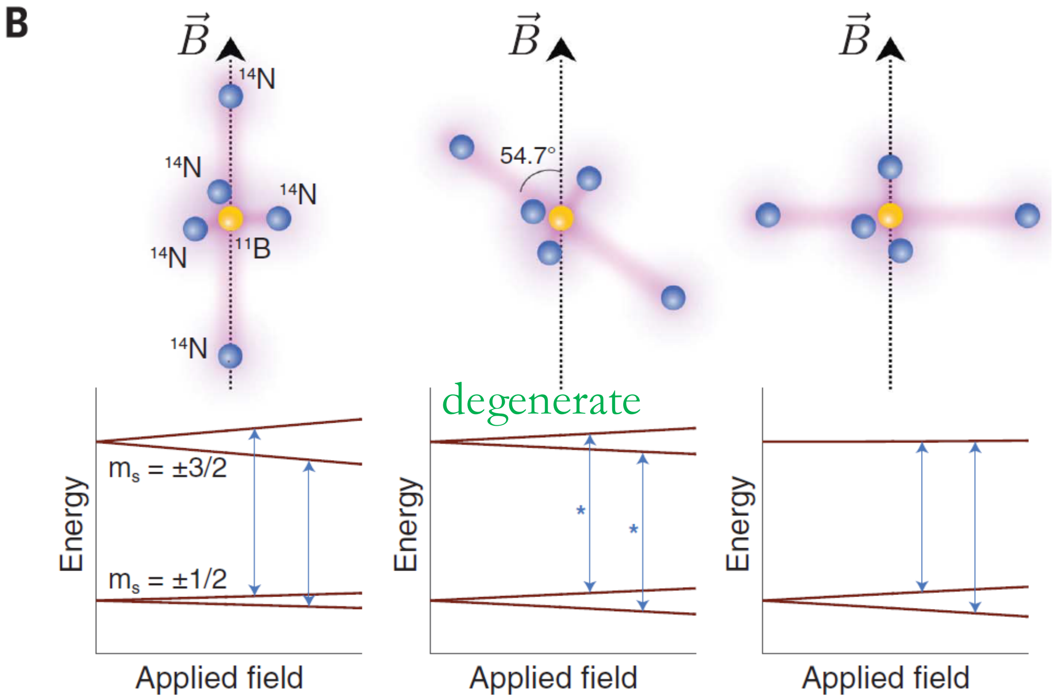

m_I = -I, -I+1, …, I-1, I

I = 3/2 I = 3

(80% ^{11}B, 20% ^{10}B)

(close to 100% ^{14}N) I = 1

honeycomb layered structure

$$E_{\pm 3/2} = \frac{h\nu_Q \rho}{2} \pm \frac{h\nu_0}{2\rho}\left[(\rho-1+\eta)^2 c_x^2 + (\rho-1-\eta)^2 c_y^2 + (2+\rho)^2 c_z^2\right]^{1/2}$$

$$E_{\pm 1/2} = -\frac{h\nu_Q \rho}{2} \pm \frac{h\nu_0}{2\rho}\left[(\rho+1-\eta)^2 c_x^2 + (\rho+1+\eta)^2 c_y^2 + (2-\rho)^2 c_z^2\right]^{1/2}$$

B. H. Suits, Handbook of Applied Solid State Spectroscopy (Springer, New York, USA, 2006).

Pulse sequence:

measure individual Fourier components of NMR

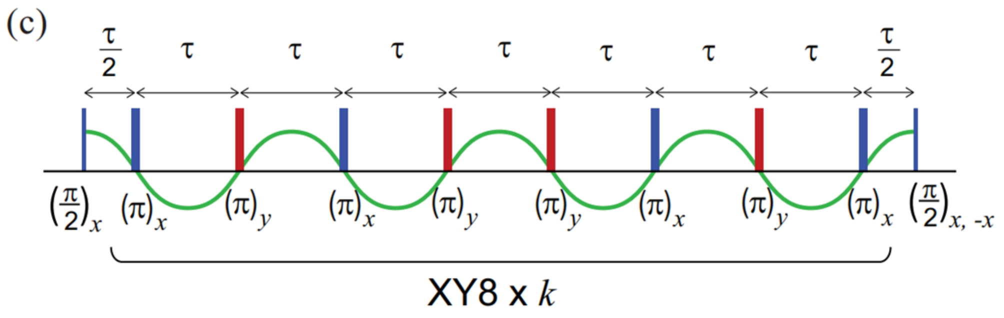

Modified: separated by identical free evolution intervals

modified XY8-371, 251···

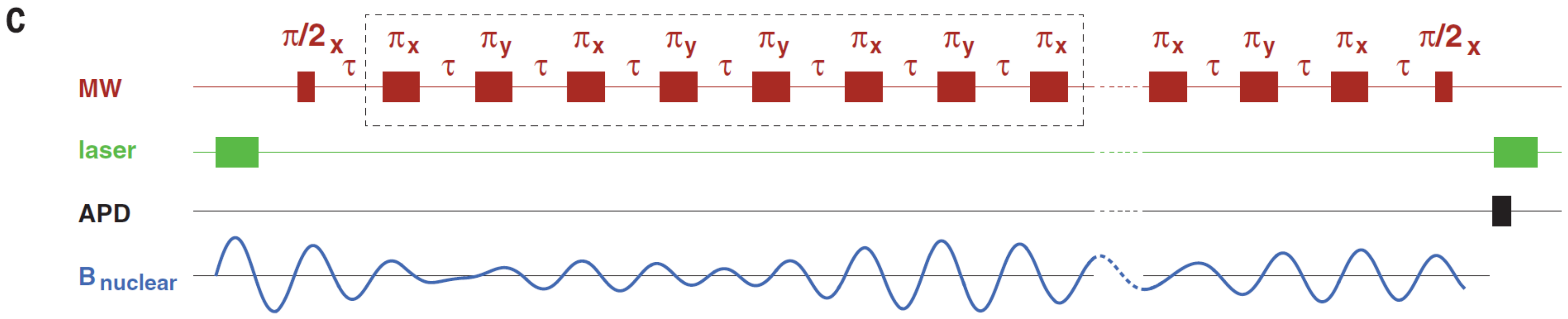

detected phase signal stored on the populations of NV dressed states

effective B_{ac} detected in a frequency-selective manner

Repetition of this sequence at different modulation frequencies yields the NQR spectrum

NQR spectroscopy of h-BN

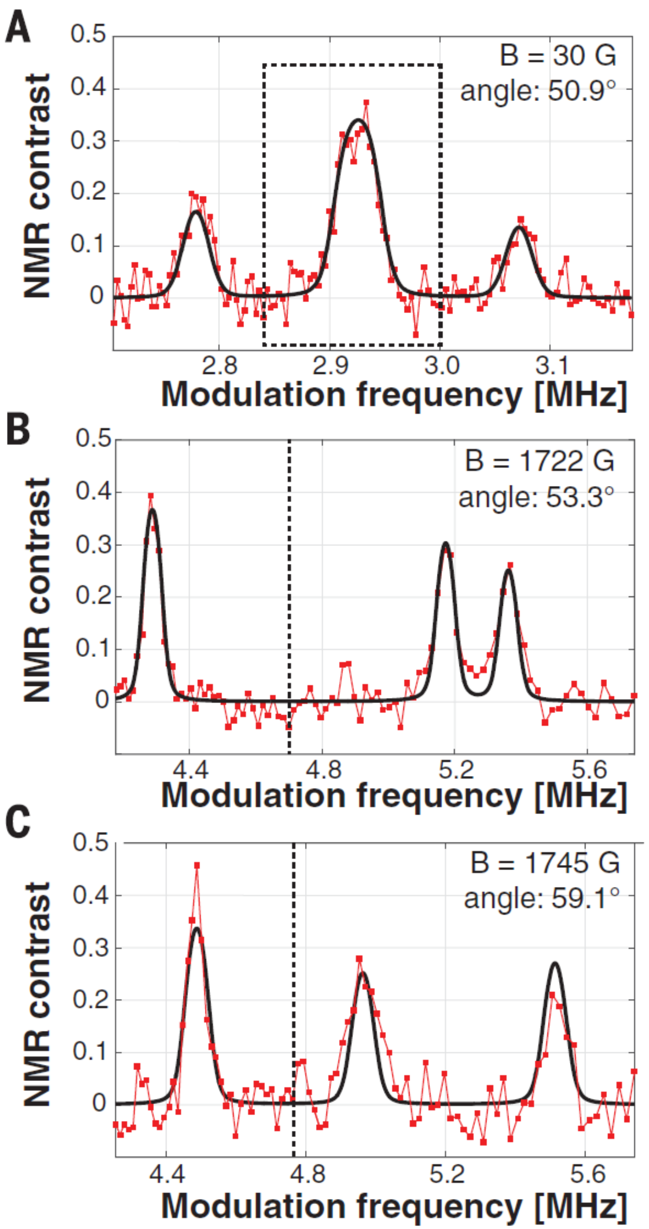

Satellite peaks: dipole-forbidden transitions become weakly allowed due to mixing by the **B** component perpendicular to the h-BN principal axis